Supplementary Materials for

Principle and Applications of Peak Force Infrared Microscopy

Le Wang,[a†] Haomin Wang [a†] and Xiaoji G. Xu *[a]

[a] Department of Chemistry, Lehigh University, Bethlehem, PA, 18015, USA.
† These authors contributed equally to this work.

The buildup of TIR-PFIR

Selections of TIR prisms and focusing elements

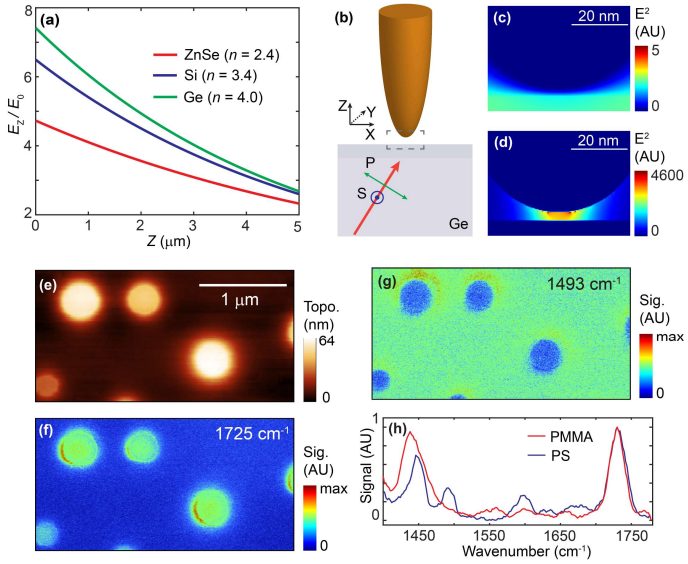

Fig. S1 TIR enhancement and demonstration of TIR-PFIR. (a) Calculated TIR field enhancements of three common TIR materials. E_Z/E_0 is enhancement factor of the *Z*-component of the evanescent field, and Z is the distance from the prism/air interface to the air. The incident wavelength is set to 6.25 μm (1600 cm^{-1}). Incident angles are set close to critical angles, which are 24.7°, 17.2°, and 14.6° for ZnSe, Si, and Ge, respectively. (b) The configuration used in the FDTD simulation. The AFM tip is modeled as a gold cone with an end radius of 30 nm. The tip-sample distance is 5 nm. A plane wave of 6.25 μm (1600 cm^{-1}) is used as the incident wave with an incident angle of 15°. The polarization of the incident wave is set to either s (out-of-plane) or p (in-plane). Field-enhancement at Ge/air interface with s-polarization is shown in (c), and with p-polarization is shown in (d). The field intensity (E^2) is represented by the false color map. (e) Topography of PS:PMMA polymer blend film. (f-g) TIR-PFIR images at absorbing frequencies of PMMA (1725 cm^{-1}) and PS (1493 cm^{-1}), respectively. (h) Point spectra collected from PMMA (red) and PS (blue) domains. (e-h) are adapted from ref. 5 with permissions.

Both TIR prism and focusing elements (e.g., IR lens and objective) need to be carefully selected to ensure a proper signal level and repeatability. Several factors such as performance, cost, availability, reproducibility, and functionality should be considered in choosing a good TIR prism. ZnSe prisms and crystals are popularly used in TIR configurations because they hold a wide IR-transparent window (3 – 12 μm) and are transparent in the visible range, facilitating an easier optical alignment using another visible laser as a guide. Other common prisms include Ge and Si; both are opaque to the visible light. The performance of three prisms can be estimated and compared using the field amplitude and the 1/*e* decay length of the generated evanescent field, which are functions of refractive indices and the incident angle.[3] The results are plotted in Figure S1a. It is evident that the Ge provides the best energy delivery near the interface. Like ZnSe and Si, Ge surface can be chemically functionalized to bind specific analytes.[4] On the other hand, Ge has a wider mid-IR-transparent window (3 – 12 μm) than Si (1.2 – 7 μm). Therefore, Ge prism was chosen as the substrate in our proof-of-principle TIR-PFIR setup described in Reference [5].

The optical path of the TIR-PFIR setup should adapt to the critical angle of the selected TIR prism to achieve the maximal intensity of the evanescent field. The IR beam is focused before entering the TIR prism. Given the finite size of the prism, the short and tight focus is difficult to achieve. Consequently, a relatively loose focus is formed on the Ge/air interface. A less tight focus means that the alignment of the TIR configuration is less stringent than that of a tight focus in side-illumination geometry. On the other hand, the fluence reduction caused by the loose focus is compensated by the strong tip-enhancement in the

evanescent field. In our TIR-PFIR demonstration, we adopted the Ge lens (Edmund Optics, focal length = 2.5 cm) as the focusing element since it is easily mountable and light-weighted, which allows for further fine-tuning of the incident angle.

Light polarization

Most AFM-IRs use p-polarized light (polarized along the tip axis) to shine the tip-sample region. In side-illumination, the p-polarization can maximize the plasmonic enhancement provided by the vertical tip dipole.[6] The same rule applies to the TIR illumination. Figures S1b-d show finite-difference time-domain (FDTD) simulation results for tip-enhancements excited by s- and p-polarized light under the same TIR configuration at the Ge/air interface. Because of the mismatch between the s-polarization and the tip dipole, no tip-enhancement can be established when using s-polarization (Figure S1c). In contrast, an enhancement factor of ~5000 is observed within the gap between the tip and sample with p-polarized light (Figure S1d). Therefore, p-polarization should be preferably used in the TIR-PFIR setup to achieve maximal tip-enhancement, as well as high sensitivity and nanoscale resolution.

Alignment and signal optimization of TIR-PFIR microscope

We used the Bruker Bioscope Catalyst AFM as the platform for the demonstration of TIR-PFIR. The piezo-scanning stage of this AFM can be elevated into the mid-air, which leaves a large open space at the bottom to install optomechanical parts for the TIR configuration. Moreover, the stage-scan mechanism ensures the XY location of the tip to be fixed in space. The Z position of the tip is determined by the sample height, which is also a fixed value for each Ge prism. In principle, other AFM models with similar designs could also be integrated into TIR-PFIR with slight modifications.

Once the XYZ position of the AFM tip is known, the next step is to align the optical path such that the IR beam can be focused onto the small Ge surface right underneath the tip. However, this alignment step is not as straightforward as in regular PFIR, where a visible He-Ne laser (632.8 nm) is made colinear with the IR beam and used as a guide. Because both Ge lens and prism are opaque in the visible range, another reference is needed to examine the quality of the alignment.

The reference of choice is the photoacoustic (PA) vibration of the cantilever. PA waves are generated when the sample absorbs laser pulses and is repetitively heated up.[7] The AFM cantilever can act as an acoustic transducer that picks up and detects PA waves. If the repetition rate of IR pulses matches the oscillation frequency of the cantilever, the free oscillation of the cantilever will be enhanced, leading to resonance-enhanced oscillations of the cantilever.

In TIR-PFIR alignment, to obtain large PA signals, a thick and homogenous PMMA layer (~500 nm) is deposited on the Ge surface and used as a standard sample. A cantilever with an oscillation frequency of Ω (usually from several tens of to hundreds of kHz) is retracted from the sample surface by 20~40 μm and used as a transducer. IR pulses are tuned to PMMA absorption (e.g., 1725 cm^{-1}), and the repetition rate is set to match Ω. The oscillation amplitude of the cantilever at the same frequency A(Ω) is monitored by a lock-in amplifier. For a coarse alignment, the position of the focus spot is adjusted in XYZ to reach maximal A(Ω). To increase the reproducibility and stability, all optomechanical parts underneath the AFM sample stage are placed on a 2D translational stage which moves in X and Y; the Ge lens is mounted on another translational stage that permits the Z optimization of the IR focus.

After the coarse alignment, the Ge prism with the standard sample is replaced by another prism with a sample of interest. The AFM tip is then engaged onto the sample surface to start PFIR measurement. Signal optimization can be achieved by slightly tuning the XYZ stage while maximizing the PFIR signal. To reduce the irreproducibility of switching to a different Ge prism, the coarse alignment can also be performed with known samples deposited on the same prism surface. For example, in the measurement of hexagonal boron nitride flakes, the AFM cantilever is first placed on top of a thick flake with large PA signals for the coarse alignment. Then, the sample stage is moved so that a thin flake of interest is placed underneath the cantilever for the final optimization and measurement of phonon polariton patterns.

Proof-of-principle demonstration

Owing to the broad compatibility of PFT mode, samples with various surface properties (e.g., soft matters, adhesive surfaces, and hard samples) could be spectroscopically investigated by TIR-PFIR. In Figures S1e-h, nanoscale domains of PS:PMMA blends are chemically mapped and distinguished. Point spectra collected at different domains (Figure S1h) show distinctive spectra features of PS and PMMA, respectively. These results confirm that, like regular PFIR, TIR-PFIR is capable of spectroscopically imaging features with nanoscale resolution. On diblock copolymer samples, the spatial resolution of TIR-PFIR was quantified to be 10 nm,[5] which is consistent with regular PFIR.[8, 9]

References

1. A. Dazzi, R. Prazeres, F. Glotin and J. M. Ortega, *Optics Letters*, 2005, **30**, 2388-2390.
2. H. Wang, J. M. González-Fialkowski, W. Li, Q. Xie, Y. Yu and X. G. Xu, *Analytical Chemistry*, 2021, **93**, 3567-3575.
3. M. Milosevic, *Applied Spectroscopy*, 2013, **67**, 126-131.
4. C. Weigel and R. Kellner, *Fresenius' Zeitschrift für analytische Chemie*, 1989, **335**, 663-668.
5. H. Wang, L. Wang, E. Janzen, J. H. Edgar and X. G. Xu, *Analytical Chemistry*, 2021, **93**, 731-736.
6. R. Ren, X. Chen and M. Liu, *Applied Physics Express*, 2021, **14**, 022002.
7. A. G. Bell, *American Journal of Science*, 1880, **s3-20**, 305.
8. D. S. Jakob, L. Wang, H. Wang and X. G. Xu, *Analytical Chemistry*, 2019, **91**, 8883-8890.
9. L. Wang, H. Wang, M. Wagner, Y. Yan, D. S. Jakob and X. G. Xu, *Science Advances*, 2017, **3**, e1700255.